Journal of Plant Physiology 176 (2015) 138–146

Contents lists available at ScienceDirect

Journal of Plant Physiology

journal homepage: www.elsevier.com/locate/jplph

Molecular biology

Molecular characterization of the cold- and heat-induced *Arabidopsis PXL1* gene and its potential role in transduction pathways under temperature fluctuations

Chang Gyo Jung[a], Sun-Goo Hwang[a], Yong Chan Park[a], Hyeon Mi Park[a], Dong Sub Kim[b], Duck Hwan Park[c], Cheol Seong Jang[a,*]

[a] Plant Genomics Laboratory, Department of Applied Plant Sciences, Kangwon National University, Chuncheon 200-713, Republic of Korea
[b] Advanced Radiation Technology Institute, Korea Atomic Energy Research Institute, 1266 Singjeong, Jeongeup 580-185, Jeonbuk, Republic of Korea
[c] Department of Applied Biology, College of Agriculture and Life Sciences, Kangwon National University, Chuncheon 200-713, Republic of Korea

ARTICLE INFO

Article history:
Received 1 August 2014
Received in revised form 1 January 2015
Accepted 1 January 2015
Available online 8 January 2015

Keywords:
Abiotic stress
Co-expression network
Germination
Leucine-rich repeat receptor-like kinase
Protein–protein interaction

ABSTRACT

LRR-RLK (Leucine-Rich Repeat Receptor-Like Kinase) proteins are believed to play essential roles in cell-to-cell communication during various cellular processes including development, hormone perception, and abiotic stress responses. We isolated an *LRR-RLK* gene previously named *Arabidopsis PHLOEM INTERCALATED WITH XYLEM-LIKE 1* (*AtPXL1*) and examined its expression patterns. *AtPXL1* was highly induced by cold and heat stress, but not by drought. The fluorescence signal of 35S::AtPXL1-EGFP was closely localized to the plasma membrane. A yeast two-hybrid and bimolecular fluorescence complementation assay exhibited that AtPXL1 interacts with both proteins, *A. thaliana* histidine-rich dehydrin1 (AtHIRD1) and *A. thaliana* light-harvesting protein complex I (AtLHCA1). We found that AtPXL1 possesses autophosphorylation activity and phosphorylates AtHIRD1 and AtLHCA1 in an *in vitro* assay. Subsequently, we found that the knockout line (*atpxl1*) showed hypersensitive phenotypes when subjected to cold and heat during the germination stage, while the *AtPXL1* overexpressing line as well as wild type plants showed high germination rates compared to the knockout plants. These results provide an insight into the molecular function of *AtPXL1* in the regulation of signal transduction pathways under temperature fluctuations.

Introduction

Plants have evolved to possess sophisticated mechanisms for adaptation to adverse environments at the transcriptional, post-transcriptional, and post-translational levels. A host of studies has revealed changes in regulation of their genome activity when exposed to abiotic and biotic stresses (Bartels and Sunkar, 2005; Vinocur and Altman, 2005; Yamaguchi-Shinozaki and Shinozaki, 2006). Especially, our understanding of stress-responsive signal transduction pathways has increased for the stress tolerance mechanisms in plants.

Plants exhibit a variety of responses to changes in temperature. The temperature fluctuations cause secondary stresses in subjected plants such as osmotic and oxidative stress (Vinocur and Altman, 2005). Modules of temperature-responsive genes in plants have been revealed by advanced genome-wide based tools such as micro-array and RNA sequencing (Zhang et al., 2013; Chang et al., 2014; Ishiguro et al., 2014). Though our knowledge of gene regulation under severe temperature conditions is increasing, how plants perceive temperature signals is largely unclear (Penfield, 2008).

Protein phosphorylation through post-translational modification is one of the most common and contentious cellular processes. The receptor-like kinases (RLKs) represent plasma membrane phosphoproteins, thus playing important roles in downstream signaling pathways (Nuhse et al., 2004; Johnson and Ingram, 2005). The leucine-rich repeats (LRRs) are composed of 20–29 amino-acid residues and their primary molecular function is to provide a versatile structural framework for protein–protein interactions (Kobe and Kajava, 2001). An enormous number of LRR-RLK proteins might be generated by the combination of LRR and RLK domains followed by genome duplication in plants (Hwang et al., 2011). For example, at least 216 and 165 members, respectively, of the *Arabidopsis LRR-RLK* gene family were reported in other studies (Shiu and Bleecker, 2001; Hwang et al., 2011).

Abbreviations: GO, gene ontology; LRR-RLK, leucine-rich repeat receptor-like kinase; WGCNA, weighted correlation network analysis.

* Corresponding author. Tel.: +82 33 250 6416; fax: +82 33 244 6410.
E-mail address: csjang@kangwon.ac.kr (C.S. Jang).

http://dx.doi.org/10.1016/j.jplph.2015.01.001
0176-1617/

LRR-RLKs are believed to play essential roles in cell-to-cell communication during development, hormone perception, and abiotic stress responses (Torii, 2004). The *Arabidopsis CLAVATA1* (*CLV1*) gene, which encodes a LRR-RLK, functions as a signal transduction component associated with the communication of cell division and/or differentiation signals in the surface cell layers of the meristem (Clark et al., 1997). Another example is the brassinosteroid-insensitive 1 (BRI1) protein, which is a LRR-RLK and plays an important role in the BR-signaling pathway through interaction with BRI-associated receptor kinase-1 (BAK1) (Li and Chory, 1997; Li et al., 2002). Recent study revealed that a *LRR-RLK* gene from *Glycine soja* is expressed under cold stress but not salinity and ABA stress, and that overexpression of the gene enhances the plants' tolerance to cold stress (Yang et al., 2014). However, even though putative molecular functions have been suggested, a large number of *LRR-RLK* genes remain unknown.

Previously, we identified an *Arabidopsis LRR-RLK* gene family using *in silico* analysis and examined its expression patterns *via* a microarray dataset (Hwang et al., 2011). We further characterized the *AtPXL1* (*Arabidopsis thaliana PHLOEM INTERCALATED WITH XYLEM-LIKE 1*, AT1G08590) gene in order to evaluate its expression under abiotic stresses and innate roles, *e.g.* autophosphorylation and transphosphorylation, of its substrates. Furthermore, seed germination of heterogeneous overexpressing and knockout plants were examined under cold and heat treatments.

Materials and methods

Plant materials and growth

Arabidopsis thaliana (L.) Heynh., ecotype Columbia (Col-0), seeds were surface-sterilized with vapor-phase sterilization (Clough and Bent, 1998). The sterilized seeds were imbibed in water for 3 d and grown vertically on Murashige and Skoog (MS) agar plates. The seeds were grown in a photoperiod-controlled growth chamber (16 h/8 h day/night) at 22 °C with 70% relative humidity. *Arabidopsis* seeds with T-DNA insertion in the *AtPXL1* gene (SALK_001782 line for *atpxl1*) were obtained from the Arabidopsis Biological Resource Center (ABRC, Ohio State University, Columbus, OH, USA). The T_4 generation homozygous for *atpxl1* was identified by PCR. Tissue samples including roots, shoot, leaves, and inflorescences were harvested from 4-weeks old plants. The *AtPXL1* gene was inserted into the *35S::EGFP* vector (Lim et al., 2013) with appropriate restriction enzymes, and thus transformed into *Arabidopsis* by the floral dip method (Zhang et al., 2006). The method for transformed seedling selection was previously described by Jung et al. (2012).

RNA analyses and abiotic stress treatments

Total RNAs were isolated using TRIzol (Invitrogen, USA). For quantitative real-time PCR (qRT-PCR) analysis, the first-strand cDNA was synthesized using the PrimeScript™ RT-PCR kit (Takara Bio, Japan). qPCR was performed using a CFX connect Real-time PCR (Bio-Rad, USA) and TOPreal™ qPCR 2× PreMIX (Enzynomics, Korea). The *Arabidopsis actin2* (*AtActinII*, AT3G18780) gene was used as the internal control. The relative mRNA levels were calculated using the $2\text{-}^{DDC}{}_{T}$ comparative method in the gene expression analysis software in Bio-Rad CFX Manager (Bio-Rad). The following typical profile was used for all qRT-PCR reactions: 95 °C for 15 min, 45 cycles of 95 °C for 20 s, 60 °C for 20 s and 72 °C 30 s with melting curve analysis. The reliable reference genes, such as *AtDREB2A* (At5g05410), *AtCBF1* (At4g25490), and *AtHSP101* (At1g74310), were also used as positive controls to validate plants subjected to each stress treatment of drought, cold, and heat, respectively. To determine dehydration response, three weeks old *Arabidopsis* seedlings grown on MS agar plates were dehydrated on Parafilm. To measure changes in the expression levels of reliable reference genes in stress-treated plants, *Arabidopsis* seeds were grown on 1/2 MS agar plates in a climate-controlled room under 16 h of light at 24 °C for 2 weeks. Two-week-old *Arabidopsis* seedlings were exposed to 12 °C for cold treatment or 42 °C for heat treatment for different times (1, 3, 5, 10, or 24 h). Gene-specific primers are listed in Supplement Table 1.

Subcellular localization

To observe the subcellular localization, each of the full-length cDNAs was introduced into the *35S::EGFP* vector. Transient expression was performed by agroinfiltration as described previously (Jung et al., 2012). Co-localizations were performed using the mCherry-labeled PM marker (PM-rk; CD3-1007) kindly provided by the ABRC (Arabidopsis Biological Resource Center) stock center (Nelson et al., 2007). Fluorescent imaging was performed using the LSM 510 META NLO system (Carl Zeiss, Germany) at the Korea Basic Science Institute Chuncheon Center, Republic of Korea.

Protein expression and in vitro kinase assay

The kinase domain of *AtPXL1* cDNAs and interacting partners were inserted into the pMAL-c5X vector for protein expression in the SoluBL21™ *E. coli* strain (Genlantis, San Diego, CA, USA). Recombinant proteins were tagged with MBP (Maltose Binding Protein) and then purified using amylose resin according to the manufacturer's recommendation (New England BioLabs, Ipswich, MA, USA). Protein kinase activity assay was performed as described previously (Li et al., 2002) with some modifications. Each reaction was performed in a total volume of 20 μL with 2 μg of each protein, kinase buffer (50 mM HEPES, pH 7.4, 10 mM $MgCl_2$, 10 mM $MnCl_2$, 1 mM DTT, and 3 μL [γ-^{32}P] ATP) for 20 min at 25 °C. The reaction was terminated by adding 4 μL 6× SDS sample buffer, incubated for 30 min at 70 °C, and run on 10% SDS-polyacrylamide gel electrophoresis. The gel was then stained, de-stained, dried, and autoradiographed.

Yeast two-hybrid analysis (Y2H)

An *Arabidopsis* cDNA library in the pGADT7-Rec was generated from gamma-ray irradiated *Arabidopsis* plants. AtPXL1KD was fused to the *pGBKT7-BD* vector. A library screening for proteins that interact with AtPXL1KD was conducted according to the manufacturer's recommendation (Make Your Own "Mate & Plate™" Library System; Matchmaker™ Gold Yeast Two-Hybrid System; Yeastmaker™ Yeast Transformation System 2, Clontech, Palo Alto, CA, USA). A total of 97 yeast transformants were selected as approximately 1×10^8 independent clones were screened on SD (Synthetic Dextrose) medium lacking Leu and Trp with 40 μg/mL X-α-Gal and 125 ng/mL Aureobasidin A (DDO/X/A). These yeast colonies were then patched onto plates lacking Ade, His, Leu, and Trp with 40 μg/mL X-α-Gal and 125 ng/mL Aureobasidin A (QDO/X/A).

Bimolecular fluorescence complementation (BiFC) assay

The full-length *AtPXL1* cDNAs and interacting partners were fused into *35S::c-Myc-SPYNE(R)* and *35S::HA-SPYCE(M)* vectors, respectively. For transient assay, each construct together with the p19 silencing suppressor construct was then infiltrated into the abaxial side of the 4-week old *Nicotiana benthamiana* leaves using

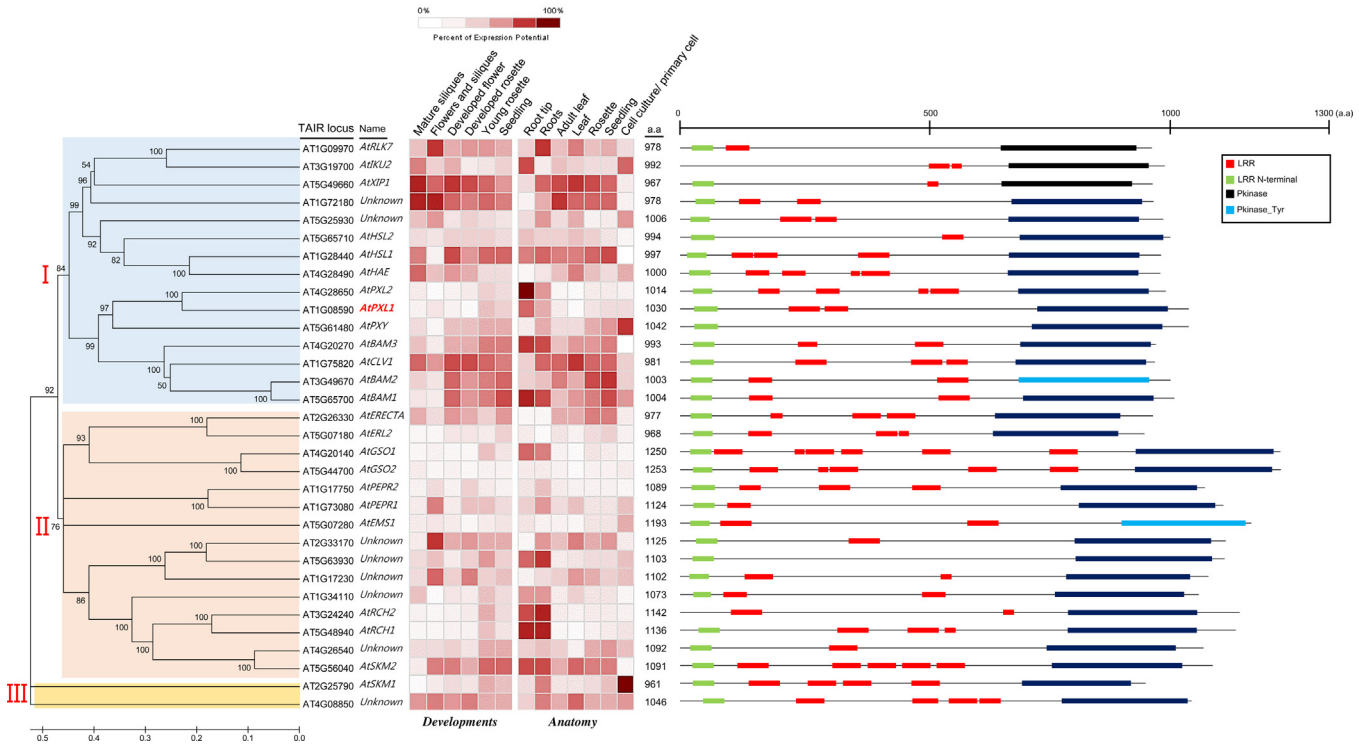

Fig. 1. *In silico* analysis of *AtPXL1* paralogs in *Arabidopsis*. The phylogenetic tree was constructed by ClustalW with neighbor joining method. Box colors represent different groups. Expression patterns were analyzed at different development stages and in various tissues *via* GENEVESTIGATOR. Domain structures of these genes were retrieved from the Pfam database. a.a. indicates amino acid length.

a 1-mL syringe. The transient expressed leaves were observed by confocal microscopy after 3 d.

Germination assays under stress conditions

In order to evaluate the effect of heat stress on germination, sterilized seeds incubated for 3 d at 4 °C were transferred into PCR tubes. Heat stress was performed for 1 h at temperatures ranging from 42 °C to 55 °C using a C1000 gradient PCR machine (Bio-Rad). The samples were subsequently transferred to half-strength MS medium containing 1% sucrose for 6 d, at which point germination was scored. To determine the effect of cold stress on seed germination, MS agar plates were placed in growth chamber maintained at 12 °C under white light for 8 d. The seeds were considered to have germinated when the radicle protruded. Expression of *AtPXL1* mRNA in independent plants (wild-type, *atpxl1*, and *35S::AtPXL1-EGFP*) was examined by RT-PCR using gene-specific primers.

Phylogenetic analysis and co-expressing modules of AtPXL1

The amino acids for genes homologous with AtPXL1 were retrieved from Phytozome (Goodstein et al., 2012). Phylogenetic analysis was performed with ClustalW with neighbor-joining algorithm (Larkin et al., 2007). Expression pattern analysis of genes was evaluated at different development stages and in various tissues by GENEVESTIGATOR (Hruz et al., 2008). Additionally, the domain structures of amino acids in each gene were retrieved from the Pfam database (Sonnhammer et al., 1997). To analyze the putative functional relationship of *AtPXL1*, co-expressing modules were determined in the integrated microarray dataset by R package WGCNA with dynamicTreeCut R package, following the procedure described by Hwang et al. (2014).

Results

Phylogenetic analysis and gene expression patterns of AtPXL1

We have previously reported the evolutionary dynamics of *LRR-RLKs* in rice and *Arabidopsis* by comparative analysis and identified high functional conservations among several tentative orthologous genes such as AT1G08590 and Os01g10900 induced by gamma ray irradiation (Hwang et al., 2011). The gene (AT1G08590) previously named *AtPXL1* (Fisher and Turner, 2007) was selected for further study of the *Arabidopsis LRR-RLK* genes. To study evolutionary relationship of *AtPXL1*, we have retrieved its homologous genes by Phytozome (Goodstein et al., 2012) (Fig. 1). A total of 31 genes were isolated as the homologs of *AtPXL1* and divided into three groups. Protein domain analysis revealed that 27 of 31 LRR-RLKs tested harbor LRR domain(s) and protein kinase domain (Fig. 1). Two genes, AT3G49670 (*AtBAM2*) and AT5G07280 (*AtEMS1*), showed a type of protein kinase domain (Pkinase_Tyr) not found in other genes. To examine the gene expression patterns at different development stages and in various tissues, we have determined the expression potential of homologous genes with *AtPXL1* based on a microarray database using GENEVESTIGATOR (Hruz et al., 2008). Most of the members of Group I were induced at various development stages and in various tissues, while those of group II were relatively not significantly induced in both. The expression of *AtPXL1* was significantly induced in roots and tips. The microarray data were consistent with our quantitative RT-PCR results that detected the highest expression levels in roots (Fig. S1).

We found that the expression of *AtPXL1* was increased in response to gamma-ray irradiation (data not shown). Therefore, we examined the expression patterns of *AtPXL1* against other abiotic stresses such as drought, cold, and heat treatments (Fig. 2A). The gene expression levels of *AtPXL1* were strongly

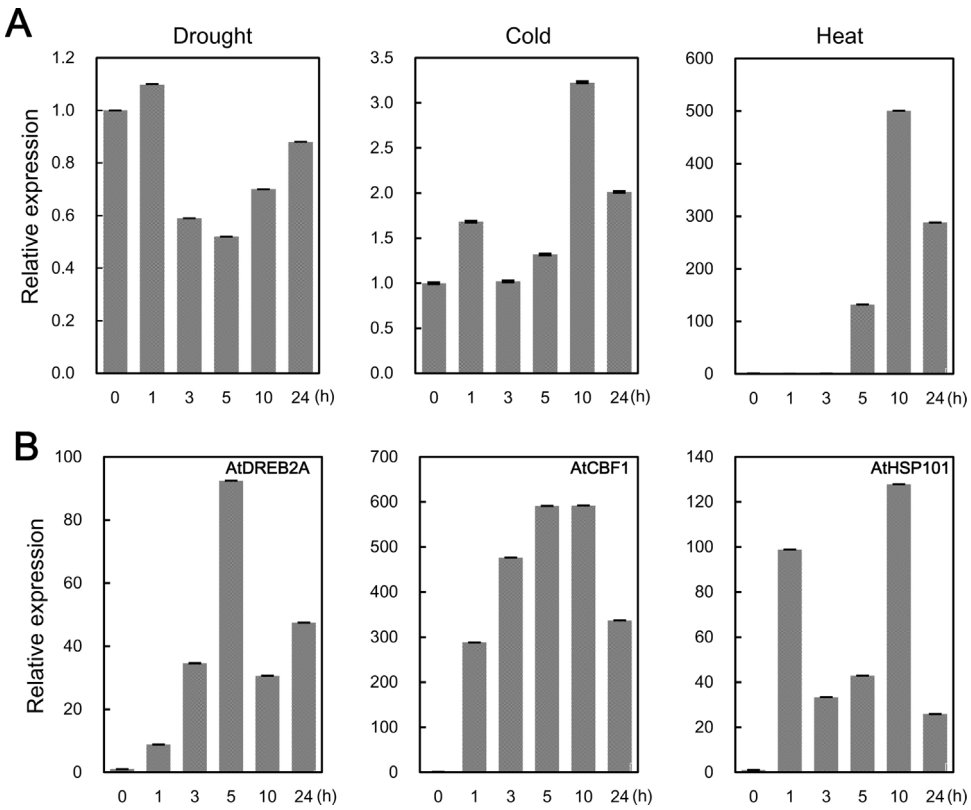

Fig. 2. (A) Expression patterns of *AtPXL1* under different abiotic stresses. Total RNAs were extracted from 3-week-old wild type plants subjected to three abiotic stresses: drought (air-dried), cold (4 °C), and heat (42 °C). *AtActinII* (AT3G18780) was used as an internal control. (B) *AtDREB2A*, *AtCBF1*, *AtHSP101* were used as reliable stress marker genes for each abiotic treatment, respectively. Data represent the mean of three independent samples ± standard deviation.

increased from 5 h until 24 h of heat stress, slightly increased at 3 h of cold treatment, and steadily expressed in response to drought treatment. To determine whether plants subjected to abiotic stresses, we employed stress-responsive genes such as *AtDREB2A* (Sakuma et al., 2006) for drought, *AtCBF1* (Kendall et al., 2011) for cold, and *AtHSP101* (Pecinka et al., 2010) for heat. As expected, these genes highly increased their expression levels from 1 h to 24 h of drought, cold, and heat stress (Fig. 2B).

Subcellular localization of AtPXL1

To examine the subcellular localization of AtPXL1 protein, full-length AtPXL1 was fused to the C-terminus of EGFP under the control of the CaMV35S promoter. The empty vector (35S::EGFP) was used as a control signal (Fig. 3A). The green fluorescence of 35S::AtPXL1-EGFP was localized to the plasma membrane (Fig. 3A). To confirm the localization of 35S::AtPXL1-EGFP, a plasma membrane marker protein, PM-rk-mCherry, was used in this study. Both proteins were co-expressed in tobacco leaves for 3 d. We found that both fluorescent signals closely overlapped with each other, confirming the plasma membrane localization of *AtPXL1*.

Protein–protein interactions with AtPXL1

In order to screen for proteins interacting with AtPXL1, we performed Y2H. We obtained 97 putative positive colonies from the first screening in DDO/X/A medium on the basis of beta-galactosidase activity (data not shown). According to the assessment of positive interactions on both DDO/X/A and QDO/X/A plates, 18 positive colonies exhibited strong protein–protein interactions with AtPXL1 (Fig. S2). We also obtained the coding sequences of gene fragments by sequencing, and then identified the gene names and annotations by a BLAST search. To understand the protein–protein interaction partners of AtPXL1 where such proteins are specifically located, their putative subcellular localizations were retrieved from TAIR (The Arabidopsis Information Resource; http://www.arabidopsis.org) database. Approximately 55% (10 out of 18) of their subcellular localizations were predicted to be localized in the chloroplast (Fig. S2). This result suggested that AtPXL1 may play a role in chloroplast function.

To identify the functional relationship between AtPXL1 and its interacting partners associated with the chloroplast, we subsequently chose two genes for further study, *i.e.*, AT1G54410 (*A. thaliana* histidine-rich dehydrin) whose molecular mass is 11 kD, previously named *AtHIRD11* by Hara et al. (2011) and AT3G54890 (*A. thaliana* light-harvesting protein complex A I), *AtLHCA1* by Umate (2010). Both partner recombinant proteins were also fused to the C-terminus of EGFP under the control of CaMV 35S promoters that were transiently expressed in tobacco leaves for 3 d. However, the fluorescence signal of AtLHCA1-EGFP was localized to the chloroplasts, while the signal of AtHIRD11 was observed as spots in the cytosol (Fig. 3B).

To visualize the interactions of the partner proteins with AtPXL1 in plant cells, BiFC analysis was performed in tobacco leaves. We transiently co-expressed the mixture of each of the 35S::HA-SPYCE(M) harboring partner genes with a 35S::c-Myc-AtPXL1-SPYNE(R) construct in tobacco leaves for 3 d. Interestingly, both BiFC signals were observed at different subcellular compartments, *i.e.* the plasma membrane (AtPXL1-YFP^{C}/AtHIRD11^{N}) and chloroplast (AtPXL1-YFP^{C}/AtLHCA1^{N}) (Fig. 3C).

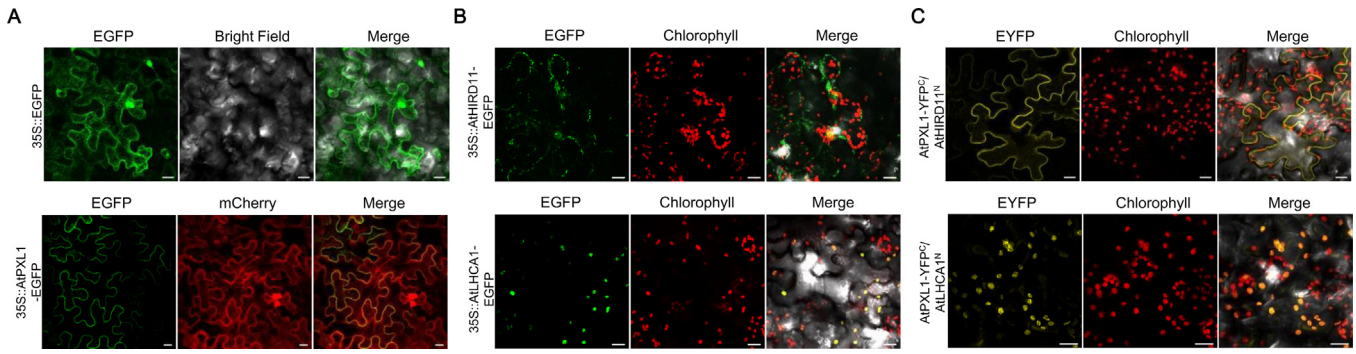

Fig. 3. Subcellular localization of AtPXL1-EGFP, AtHIRD11-EGFP, and AtLHCA1-EGFP fusion proteins and BiFC interactions of AtPXL1 with AtHIRD11 and AtLHCA1 in tobacco leaf epidermal cells. (A) Co-localization of AtPXL1-EGFP to the plasma membrane marker PM-rk-mCherry. 35S::EGFP is used as a control signal. (B) AtHIRD11. (C) AtLHCA1. Scale bar = 20 μm.

Co-expressed module analysis of AtPXL1

To study the functional relationship of *AtPXL1*, we performed co-expressed module detection analysis by using WGCNA with dynamic tree cutting algorithm (Langfelder and Horvath, 2008). A total of 208 functionally interacting genes showed high co-expressions as a module of turquoise color with *AtPXL1* (Fig. S3). According to the functional enrichment analysis of these genes, we surveyed the enriched GeneOntology (GO) functions with three categories: biological process (BP), molecular function (MF), and cellular component (CC) (Table 1). This module was significantly overrepresented in the lipid-related functions and response to oxidative stress and chemical stimulus in BP, oxidoreductase and antioxidant activity, and ion binding-related functions in MF and membrane-associated localizations in CC.

AtPXL1 phosphorylates their partner in vitro and the partners' expression in abiotic stress

The *AtPXL1* cytoplasmic domain is predicted to contain Ser/Thr protein kinase (Fig. 4A). To test whether AtPXL1 encodes an active protein kinase, the AtPXL1 cytoplasmic kinase domain (AtPXL1KD) fused with maltose binding protein (MBP) was expressed in *E. coli*, purified, and tested for the autophosphorylation activity (Fig. 4B) when incubated with [γ-^{32}P] ATP. In addition, MBP-AtBRI1KD was used as a positive control (Li et al., 2002). AtPXL1KD showed similar autophosphorylation activity compared with that of the AtBRI1KD (Fig. 4B), suggesting that the protein possesses an active kinase domain. In addition, kinase proteins were known to phosphorylate conventional substrates. The phosphorylated substrates' proteins in the gel were visualized by incubating with [γ-^{32}P] ATP and

Table 1
Enriched functions of co-expressed genes of *AtPXL1*.

Categories	GO IDs	GO terms	Percentage of genes	*p*-Value	FDR
Biological process	GO:0010876	Lipid localization	2.870813	1.40E – 08	5.40E – 06
	GO:0006979	Response to oxidative stress	4.784689	2.20E – 05	0.0044
	GO:0042221	Response to chemical stimulus	11.96172	0.00026	0.034
	GO:0006869	Lipid transport	2.870813	0.00036	0.036
	GO:0009698	Phenylpropanoid metabolic process	2.870813	0.00052	0.041
Molecular function	GO:0016684	Oxidoreductase activity, acting on peroxide as acceptor	6.220096	1.10E – 12	1.30E – 10
	GO:0004601	Peroxidase activity	6.220096	1.10E – 12	1.30E – 10
	GO:0016209	Antioxidant activity	6.220096	8.00E – 12	6.00E – 10
	GO:0020037	Heme binding	4.784689	4.50E – 10	2.60E – 08
	GO:0005506	Iron ion binding	5.263158	3.50E – 09	1.60E – 07
	GO:0046906	Tetrapyrrole binding	4.784689	9.50E – 09	3.60E – 07
	GO:0009055	Electron carrier activity	5.741627	1.50E – 07	5.00E – 06
	GO:0043169	Cation binding	14.83254	6.70E – 07	1.70E – 05
	GO:0043167	Ion binding	14.83254	6.70E – 07	1.70E – 05
	GO:0016491	Oxidoreductase activity	11.96172	7.90E – 07	1.70E – 05
	GO:0046872	Metal ion binding	14.35407	8.20E – 07	1.70E – 05
	GO:0046914	Transition metal ion binding	12.44019	1.40E – 06	2.70E – 05
	GO:0046527	Glucosyltransferase activity	2.870813	0.00014	0.0025
	GO:0003824	Catalytic activity	36.36364	0.00035	0.0057
	GO:0005488	Binding	39.23445	0.0023	0.035
Cellular component	GO:0012505	Endomembrane system	20.09569	8.30E – 07	6.70E – 05
	GO:0031225	Anchored to membrane	3.827751	0.00017	0.0054
	GO:0031224	Intrinsic to membrane	6.698565	0.0002	0.0054

Significant confidence intervals were calculated by agriGO (*p*-value < 0.05, FDR < 0.05) (Du et al., 2010).

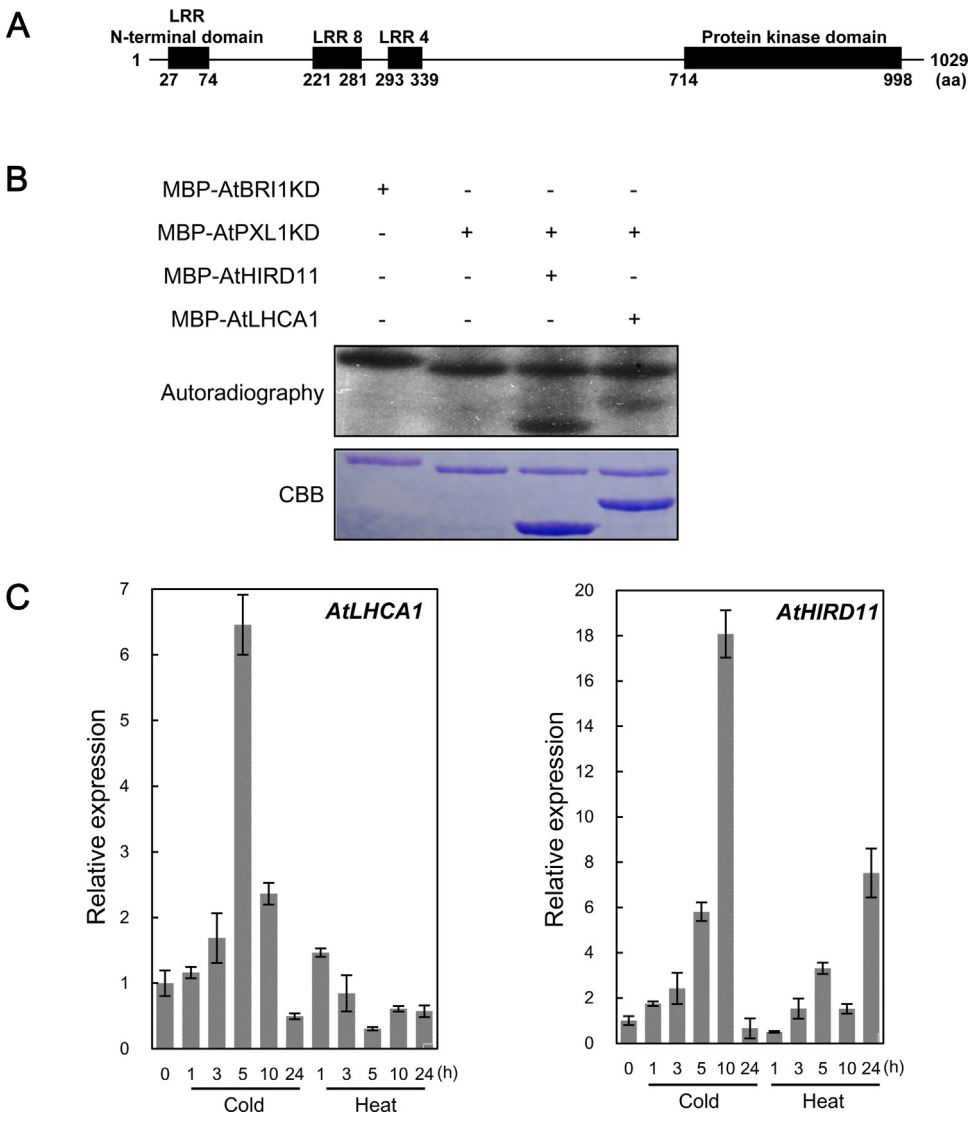

Fig. 4. *In vitro kinase assay* of the AtPXL1 protein and expression patterns of its substrates proteins, AtHICA1 and AtLHCA1. (A) Deduced amino acids of AtPXL1. (B) Autophosphorylation and transphosphorylation of AtPXL1. Proteins were separated by 9% SDS-PAGE after incubation in protein kinase buffer and [γ-32^P] ATP. Each lane represents an independent reaction. Protein abundance was indicated by CBB staining. KD, kinase domain. (C) Expression patterns of the substrates. Total RNA was extracted at the indicated times. Expression levels were normalized by *AtActinII* gene. Data represent the mean of three independent samples ± standard deviation.

then exposing the X-ray film. As shown in the kinase assay results, AtPXL1 protein's substrates including AtHIRD11 and AtLHCA1 were phosphorylated by AtPXL1 *in vitro* (Fig. 4B). This result suggested that AtPXL1 regulates the functions of the AtHIRD11 and AtLHCA1 proteins *via* phosphorylation.

We subsequently questioned expression patterns of *AtPXL1* partner genes under cold and heat treatments. Expressions of the two partner genes were clearly increased under cold stress (Fig. 4C). In the cold treatment samples, *AtHIRD11* transcripts were significantly induced until 10 h but decreased at 24 h after the treatment, while *AtLHCA1* transcripts showed the highest expression at 5 h after the treatment. In contrast, in the heat treatment samples, the expression of *AtHIRD11* significantly increased at 24 h, while the expression of *AtLHCA1* slightly decreased.

Putative roles of AtPXL1 in seed germination under cold and heat stress

Subsequently, we generated 15 *AtPXL1* overexpressing transgenic plants driven by the CaMV 35S promoter. Accumulated *AtPXL1* mRNAs in these transgenic plants were determined by the semi-quantitative RT-PCR. We selected one *35S::AtPXL1-EGFP* line for further analysis on the basis of expression. Based on the mRNA expression data given in Fig. 2, we hypothesized that *AtPXL1* involves tolerance mechanisms under cold and heat stresses. To investigate the stress response associated with *AtPXL1*, we examined the phenotypes among the wild-type (WT), knockout mutant (*atpxl1*), and overexpressing line (35S::*AtPXL1-EGFP*) under cold and heat stresses. Under normal growth condition, germination rate in WT, *atpxl1*, and *35S::AtPXL1-EGFP* reached 100% in 2 d (Fig. 5B). However, when exposed to cold and heat stress, the germination rates in the three types of plants was significantly different (Fig. 5C and D). When the seeds were subjected to 12 °C during germination, germination initiated at 3 d in all three types of plants. At 4 d, germination rates for *35S::AtPXL1-EGFP* line (86.4% ± 2.3) and WT (69.1% ± 3.8) were noticeably higher compared to that of *atpxl1* (32.1% ± 4.8). Subsequently, germination rates of *35S::AtPXL1-EGFP* and WT seeds reached 100% at 7 and 8 d, respectively. In contrast, germination rate of *atpxl1* seeds reached to only 56.8% at 8 d of cold treatment (Fig. 5D).

Under high-temperature conditions, germination of *atpxl1* seeds was suppressed, while the *35S::AtPXL1-EGFP* and WT seeds

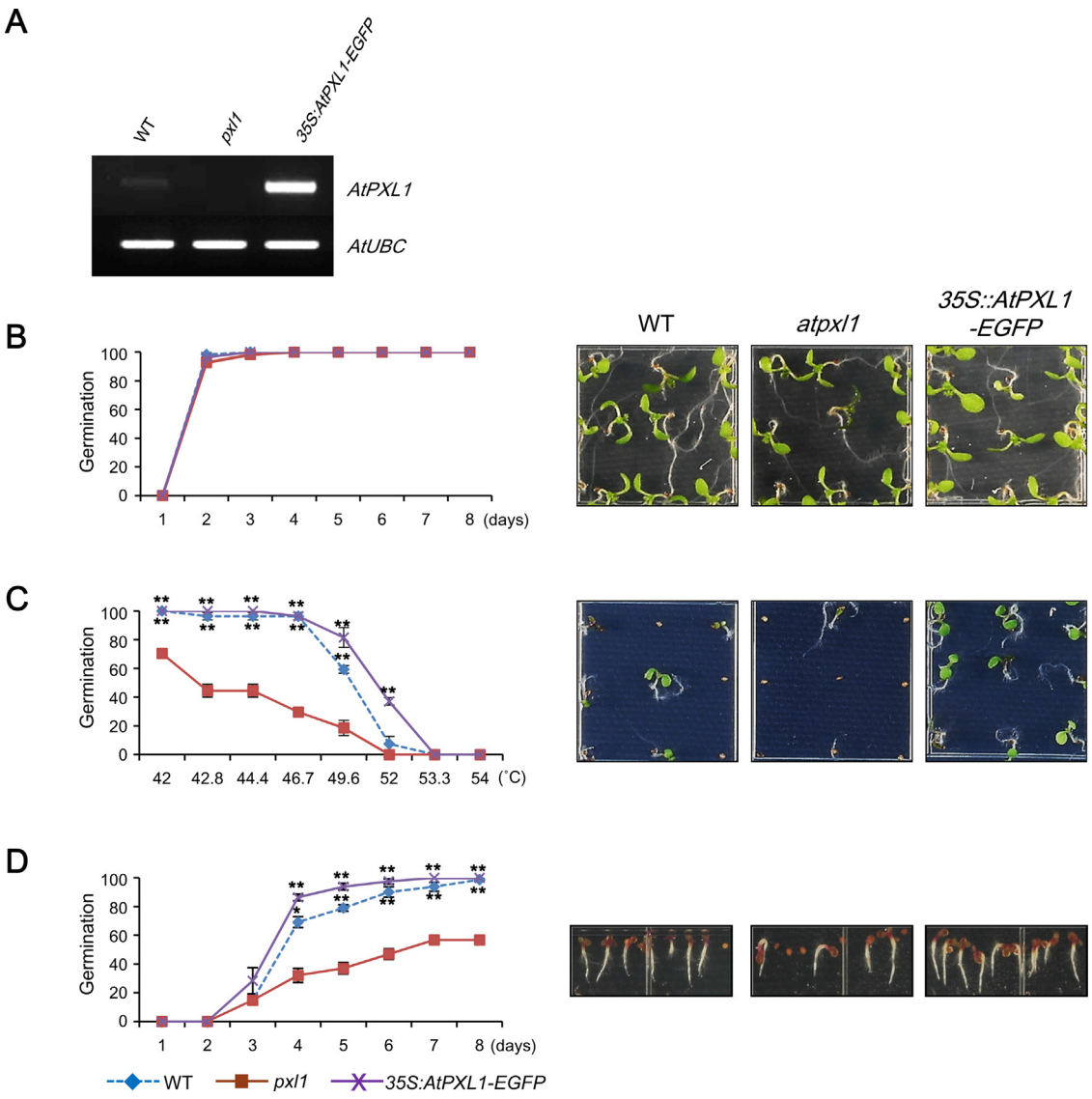

Fig. 5. Germination rates of wild-type, *atpxl1*, and *35S::AtPXL1-EGFP* overexpressing plants. (A) RT-PCR analysis of *AtPXL1* in wild-type, *atpxl1*, and *35S::AtPXL1-EGFP* overexpressing plants. *Arabidopsis UBC* (ubiquitin-conjugating enzyme) transcript levels were used as internal control. (B) Germination rates of wild-type, *atpxl1*, and *35S::AtPXL1-EGFP* plants at 24 °C. A representative image taken on day 5 after planting is shown. (C) Germination rates of wild-type, *atpxl1*, and *35S::AtPXL1-EGFP*-overexpressing plants, which were imbibed in water for 3 d and then exposed to heat shock for 1 h before plating. Seed germination was checked, and plants were photographed 6 d after plating. (D) Germination rates of wild-type, *atpxl1*, and *35S::AtPXL1-EGFP*-overexpressing plants, which were germinated at low temperature (12 °C). A representative photograph, taken on day 6 after incubating at 12 °C, is shown. Results are presented as means and standard errors from three independent experiments ($n > 27$). * and ** indicate significant differences of overexpressing transgenic lines in comparison to *atpxl1* at $p < 0.05$ and $p < 0.01$, respectively (Student's *t*-test).

were not affected. Germination of *atpxl1* seeds was low at 42 °C incubation, and it ceased with increasing incubation temperature to 52 °C or more. However, WT and *atpxl1* seeds showed approximately 100% germination rate until 46.7 °C. *35S::AtPXL1-EGFP* showed higher germination rate between 49.6 °C and 52.0 °C than *atpxl1*. In contrast, both seeds did not germinate above 53.3 °C.

Discussion

Phylogenetic analysis showed that *AtPXL1* is closely related to *AtPXY* (*A. thaliana phloem intercalated with xylem*). The *AtPXY* gene encoding an RLK are known to maintain cell polarity required for the orientation of cell division (Fisher and Turner, 2007). Previous finding that double-mutants of *atpxy* and *atpxl1* exhibited a more severe vascular phenotype even though *atpxl1* did not exhibit an obvious phenotype in the stem implies the molecular function of *AtPXL1* in vascular development (Fisher and Turner, 2007). However, its function in response to temperature fluctuation has not been reported, yet.

Our findings regarding the expression patterns in response to cold and heat conditions suggest the molecular functions in mediating signal pathways against thermal stresses. Especially, significant increase of *AtPXL1* transcripts, *e.g.*, approximately 500 fold at 10 h after heat treatment, which appears to be unusual, implies an important role of the gene in heat stress response. We found that two interaction partners *AtHIRD11* and *AtLHCA1* were highly increased during cold and cold/heat treatments, respectively. These results support our hypothesis that the *AtPXL1* gene mediates the signaling pathways against thermal stress. Dehydrin genes are believed to play important roles in plant response and adaptation to abiotic stresses, in particular dehydration and salinity as well as cold and freezing stress (Hanin et al., 2011). The

photosystem proteins such as AtLHCA1 under stress try to recover and maintain a proper defense system within the cell by increasing the ATP synthesis due to an higher demand of energy (Ozakca, 2013). Even though our study did not reveal the interacting partners controlled by AtPXL1 *in vivo*, we hypothesize that AtPXL1 regulates the functions of the AtHIRD11 and AtLHCA1 proteins through protein phosphorylation in *Arabidopsis* plants and *in vitro*.

In addition, putative functional relationship analysis revealed that *AtPXL1* was highly co-expressed with genes with functions such as response to oxidative stress (BP), oxidoreductase activity, and antioxidant activity (MF), in which the predicted subcellular localizations of co-expressed genes were mainly associated with nucleus (21.53%) and chloroplast (21.53%) (Table 1, Fig. S3). The results, therefore, provide fundamental clues to understanding the putative roles of *AtPXL1* in the signaling pathways against thermal stresses.

LRR-RLK genes are mainly localized to the plasma membrane due to their transmembrane domains. RLK domains are believed to play fundamental roles in activating downstream signal transduction *via* phosphorylation of active loop in the kinase domain (Yan et al., 2012). In addition, phosphorylation of the juxtamembrane regions of LRR-RLKs causes significant changes in the conformation to dock specific downstream substrates; thus, substrates phosphorylated by RLK change their subcellular localization and/or interact with other proteins for ligand-dependent cellular response (Clouse et al., 2012). We found that AtPXL1KD was autophosphorylated, and substrates such as AtHIRD11 and AtLHCA1 were phosphorylated by AtPXL1KD. In addition, the fluoresce signals of AtPXL1 and both substrates were found in plasma membrane and chloroplast, respectively. In particular, AtHIR11 exhibited altered subcellular localization from the cytosol to the plasma membrane through protein–protein interactions with AtPXL1. Even though much work is still required, the changed subcellular localizations between AtPXL1 and its substrates is indicative of the existence of different mechanisms of AtPXL1 required to regulate downstream signal transduction *via* subcellular translocation.

We found that *atpxl1* showed hypersensitive phenotypes when subjected to cold and heat treatments during the germination phase, while the *AtPXL1* overexpressing line as well as wild type plants had high germination rates compared to the knockout plants (Fig. 5). In addition, the cold stress-induced reference genes exhibited strong changes in gene expression in both cold-treated *Arabidopsis* plants, including WT, and overexpressing lines and knockout plants of *AtPXL1* (Fig. S4). *AtHsp101* was also induced in both cold-treated *Arabidopsis* plants, while *AtHsa32* was induced only in WT plants by cold stress (Fig. S4). In the post-germination test, however, no significant differences were observed among wild type, overexpressing line, and knockout plants. These observations suggested that *AtPXL1* positively mediates signal transduction associated with cold and heat stress, at least during the germination stage. Moreover, different gene expression patterns of reliable reference genes showed that *AtPXL1* sends a signal to downstream genes involved in cold- and heat-stress response pathways.

Conclusions

In this study, we isolated one *LRR-RLK* gene, *AtPXL1*, and examined its expression patterns, subcellular localization, protein–protein interactions *via* Y2H and BiFC and kinase assay, and functions *via* induced over-expression or dysfunction *via* T-DNA inserted knockout. These results provide insight into the molecular function of *AtPXL1* in the regulation of signal transduction pathways in fluctuating temperatures.

Acknowledgements

This work was supported by a grant from the Korea Atomic Energy Research Institute (KAERI) and the Ministry of Education, Science, and Technology (MEST), Republic of Korea.

Appendix A. Supplementary data

Supplementary data associated with this article can be found, in the online version, at http://dx.doi.org/10.1016/j.jplph.2015.01.001.

References

Bartels D, Sunkar R. Drought and salt tolerance in plants. Crit Rev Plant Sci 2005;24:23–58.
Chang CY, Lin WD, Tu SL. Genome-wide analysis of heat-sensitive alternative splicing in *Physcomitrella patens*. Plant Physiol 2014;165:826–40.
Clark SE, Williams RW, Meyerowitz EM. The CLAVATA1 gene encodes a putative receptor kinase that controls shoot and floral meristem size in *Arabidopsis*. Cell 1997;89:575–85.
Clough SJ, Bent AF. Floral dip: a simplified method for Agrobacterium-mediated transformation of *Arabidopsis thaliana*. Plant J 1998;16:735–43.
Clouse SD, Goshe MB, Huber SC. Phosphorylation and RLK signaling. In: Anonymous receptor-Like kinases in Plants to Receptor-like Kinases in Plants. Springer Berlin Heidelberg; 2012. p. 227–51.
Du Z, Zhou X, Ling Y, Zhang Z, Su Z. agriGO: a GO analysis toolkit for the agricultural community. Nucleic Acids Res 2010;38:W64–70.
Fisher K, Turner S. PXY a receptor-like kinase essential for maintaining polarity during plant vascular-tissue development. Curr Biol 2007;17:1061–6.
Goodstein DM, Shu S, Howson R, Neupane R, Hayes RD, Fazo J, et al. Phytozome: a comparative platform for green plant genomics. Nucleic Acids Res 2012;40:D1178–86.
Hanin M, Brini F, Ebel C, Toda Y, Takeda S, Masmoudi K. Plant dehydrins and stress tolerance: versatile proteins for complex mechanisms. Plant Signaling Behav 2011;6:1503–9.
Hara M, Shinoda Y, Kubo M, Kashima D, Takahashi I, Kato T, et al. Biochemical characterization of the *Arabidopsis* KS-type dehydrin protein, whose gene expression is constitutively abundant rather than stress dependent. Acta Physiol Plant 2011;33:2103–16.
Hruz T, Laule O, Szabo G, Wessendorp F, Bleuler S, Oertle L, et al. Genevestigator v3: a reference expression database for the meta-analysis of transcriptomes. Adv Bioinf 2008;2008:420747.
Hwang S, Kim DS, Jang CS. Comparative analysis of evolutionary dynamics of genes encoding leucine-rich repeat receptor-like kinase between rice and *Arabidopsis*. Genetica 2011;139:1023–32.
Hwang S, Kim DS, Hwang JE, Han A, Jang CS. Identification of rice genes associated with cosmic-ray response via co-expression gene network analysis. Gene 2014;541:82–91.
Ishiguro S, Ogasawara K, Fujino K, Sato Y, Kishima Y. Low temperature-responsive changes in the anther transcriptome's repeat sequences are indicative of stress sensitivity and pollen sterility in rice strains. Plant Physiol 2014;164:671–82.
Johnson KL, Ingram GC. Sending the right signals: regulating receptor kinase activity. Curr Opin Plant Biol 2005;8:648–56.
Jung CG, Lim SD, Hwang SG, Jang CS. Molecular characterization and concerted evolution of two genes encoding RING-C2 type proteins in rice. Gene 2012;505:9–18.
Kendall SL, Hellwege A, Marriot P, Whalley C, Graham IA, Penfield S. Induction of dormancy in *Arabidopsis* summer annuals requires parallel regulation of DOG1 and hormone metabolism by low temperature and CBF transcription factors. Plant Cell 2011;23:2568–80.
Kobe B, Kajava AV. The leucine-rich repeat as a protein recognition motif. Curr Opin Struct Biol 2001;11:725–32.
Langfelder P, Horvath S. WGCNA: an R package for weighted correlation network analysis. BMC Bioinf 2008;9:559.
Larkin MA, Blackshields G, Brown NP, Chenna R, McGettigan PA, McWilliam H, et al. Clustal W and Clustal X version 2.0. Bioinformatics 2007;23:2947–8.
Li J, Chory J. A putative leucine-rich repeat receptor kinase involved in brassinosteroid signal transduction. Cell 1997;90:929–38.
Li J, Wen J, Lease KA, Doke JT, Tax FE, Walker J. CBA K1, an *Arabidopsis* LRR receptor-like protein kinase, interacts with BRI1 and modulates brassinosteroid signaling. Cell 2002;110:213–22.
Lim SD, Hwang JG, Jung CG, Hwang SG, Moon JC, Jang CS. Comprehensive analysis of the rice RING E3 ligase family reveals their functional diversity in response to abiotic stress. DNA Res 2013;20:299–314.
Nelson BK, Cai X, Nebenfuhr A. A multicolored set of in vivo organelle markers for co-localization studies in *Arabidopsis* and other plants. Plant J 2007;51:1126–36.
Nuhse TS, Stensballe A, Jensen ON, Peck SC. Phosphoproteomics of the *Arabidopsis plasma* membrane and a new phosphorylation site database. Plant Cell 2004;16:2394–405.
Ozakca DU. Effect of Abiotic Stress on Photosystem I-Related Gene Transcription in Photosynthetic Organisms. Photosynthesis, Dubinsky Z (Ed.), ISBN:

978-953-51-1161-0, InTech 2013; DOI: 10.5772/55350. Available from: http://www.intechopen.com/books/photosynthesis/effect-of-abiotic-stress-on-photosystem-i-related-gene-transcription-in-photosynthetic-organisms

Pecinka A, Dinh HQ, Baubec T, Rosa M, Lettner N, Mittelsten Scheid O. Epigenetic regulation of repetitive elements is attenuated by prolonged heat stress in *Arabidopsis*. Plant Cell 2010;22:3118–29.

Penfield S. Temperature perception and signal transduction in plants. New Phytol 2008;179:615–28.

Sakuma Y, Maruyama K, Osakabe Y, Qin F, Seki M, Shinozaki K, et al. Functional analysis of an *Arabidopsis* transcription factor, DREB2A, involved in drought-responsive gene expression. Plant Cell 2006;18:1292–309.

Shiu SH, Bleecker AB. Receptor-like kinases from *Arabidopsis* form a monophyletic gene family related to animal receptor kinases. Proc Natl Acad Sci USA 2001;98:10763–8.

Sonnhammer EL, Eddy SR, Durbin R. Pfam: a comprehensive database of protein domain families based on seed alignments. Proteins: Struct Funct Genet 1997;28:405–20.

Torii KU. Leucine-rich repeat receptor kinases in plants: structure, function, and signal transduction pathways. Int Rev Cytol 2004;234:1–46.

Umate P. Genome-wide analysis of the family of light-harvesting chlorophyll a/b-binding proteins in *Arabidopsis* and rice. Plant Signaling Behav 2010;5:1537–42.

Vinocur B, Altman A. Recent advances in engineering plant tolerance to abiotic stress: achievements and limitations. Curr Opin Biotechnol 2005;16:123–32.

Yamaguchi-Shinozaki K, Shinozaki K. Transcriptional regulatory networks in cellular responses and tolerance to dehydration and cold stresses. Annu Rev Plant Biol 2006;57:781–803.

Yan L, Ma Y, Liu D, Wei X, Sun Y, Chen X, et al. Structural basis for the impact of phosphorylation on the activation of plant receptor-like kinase BAK1. Cell Res 2012;22:1304–8.

Yang L, Wu K, Gao P, Liu X, Li G, Wu Z. GsLRPK, a novel cold-activated leucine-rich repeat receptor-like protein kinase from *Glycine soja*, is a positive regulator to cold stress tolerance. Plant Sci 2014;215:19–28.

Zhang X, Rerksiri W, Liu A, Zhou X, Xiong H, Xiang J, et al. Transcriptome profile reveals heat response mechanism at molecular and metabolic levels in rice flag leaf. Gene 2013;530:185–92.

Zhang X, Henriques R, Lin SS, Niu QW, Chua NH. Agrobacterium-mediated transformation of *Arabidopsis thaliana* using the floral dip method. Nat Protoc 2006;1:641–6.